Automatic characterization of soft tissues material properties during mechanical tests

Bernardo Innocenti
Jean-Charles Larrieu
Pierre Lambert
Silvia Pianigiani

BEAMS Department, Université Libre de Bruxelles, Bruxelles, Belgium

Corresponding author:
Bernardo Innocenti
BEAMS Department,
Université Libre de Bruxelles
Avenue Roosevelt 50
1050 Bruxelles, Belgium
E-mail: bernardo.innocenti@ulb.ac.be

Summary

***Introduction*: The estimation of the non-linear viscoelastic characteristics of human soft tissues, such as ligaments and tendon, is often affected by the implemented procedure. This study aims at developing and validating a protocol, associated with a contactless and automatic procedure, enabling the determination of the material behavior and properties of any soft tissues.**
***Methods*: Several markers were drawn onto the soft tissue specimen analyzed under uniaxial tensile test. An automatic contactless procedure, that uses a camera for recording the position of the markers during the test, was developed to compute the displacement, and the force applied, enabling the calculation of the true-stress/strain curve of the material. Young's modulus and Poisson's ratio can be calculated, on demand, for selected regions of interest of the soft tissues. The repeatability and reproducibility of the procedure were analyzed. The procedure was initially tested and verified on an artificial silicone material and later applied for investigating the mechanical behavior of a pig Achilles tendon and of a human patellar tendon.**
***Results*: The procedure show a high repeatability, independent by the operator, reliability and accuracy for the tested synthetic material (with a maximum error of 3.7% for Young's modulus). Additionally, the developed protocol was also suitable for the analysis of animal and human soft tissues.**
***Conclusion*: A protocol to automatically and accurately determine material properties in soft tissues was developed, tested and validated. Such approach could successfully be implemented for the mechanical characterization of any biological soft-tissue.**
Level of evidence: V.

KEY WORDS: contactless, ligaments, young's modulus, poisson's ratio, tendons.

Introduction

In an intact human joint, soft-tissues are differently involved, enabling joint stability as well as to transmit movement and forces[1].
In order to improve the understanding of their functionality, mechanical tests on animals on human specimens' samples are commonly performed[2,3]. The results of such tests, for both physiological and pathological samples, are fundamental in order to provide clinical guidelines, to identify the mechanical impact of pathologies on human joints, to check new possible rehabilitation or surgical treatments and to deliver inputs for the development of reliable biomechanical models[4,5].
Even if several studies are already present in the literature, no agreement can be currently found for the characterization of a specific soft-tissue[3,5]. For example, it is recognized that ligaments are characterized by a non-linear viscoelastic behavior[5,6] which implies their mechanical properties increases along with the loading rate. However, they are often modeled as linear elastic elements, furthermore, the range of values that could be used to characterize their stiffness presents huge standard deviations[5,7-14].
Indeed, soft tissues have peculiar mechanical characteristics, which present technical challenges to be solved by the researchers. The difficulties in defining the correct material behavior in terms of both material model and material properties can be attributed to several factors. For instance, ligaments and tendons are often tested dissecting samples of small dimensions omitting the effect of the entire section or length of the soft-tissue or of the bony attachments. Moreover, mechanical tests are usually performed under different humidity and temperature conditions, with different applied forces and under different crosshead speeds of the machine[3,15-20].
A literature review showed that there is a lack of proven guidelines and validated techniques to be

used for characterizing soft-tissues, such as ligaments and tendons[2,3,5-7,21].

In detail, following the conventional methodology, the extremities of the dissected soft-tissue are fastened to the mechanical clamps of a tensile machine, then the distance between the clamp directly measured as output of the test. Consequently, the strain of the material can be derived, together with the stress, by using the measured force and the relative section of the sample[3,5]. However, such procedure neglects the possible material slipping inside the clamps during the test, overestimating the real strain of the material. It also does not consider the eventual mechanical variability along the material[5,7,15,19]. In fact, ligaments do not express the same behavior along their entire length and several regions could be identified in a soft tissue; for instance, the one close to the bony attachments and the middle region, are characterized by different behaviors and properties[15,20].

A correct analysis of the behavior of these different regions gives fundamental information to clinicians and engineers when they need to analyze or to investigate human joints; thus it is fundamental that their determination is extremely accurate and repeatable.

Therefore, this study aims to:

1. develop and validate a testing protocol associated with an automatic contactless procedure able to determine the material properties from a mechanical uniaxial tensile test;
2. verify the proposed testing protocol by using an artificial silicone material;
3. test the experimental protocol on biological soft-tissues.

Materials and methods

Testing protocol

The experimental protocol was subdivided into three steps:

1. specimen preparation;
2. tensile test;
3. automatic material characterization.

Initially, once the specimen was selected, several markers were directly drawn onto it (Fig. 1). Markers were drawn with waterproof dyeing in dark color to increase the contrast with respect to the analyzed material. To make the markers all similar, a square-shaped guide was used to obtain square markers of 4 mm side. Special care was dedicated to this phase as it was important to not compromise the integrity of the material. The choice of using markers was decided to avoid any disturbances during the registration, and therefore the measurement, of the displacements. Since the material was deformed during the tensile test, if solid or invasive markers were used, they would have had an impact on the behavior of the material, such as changing its properties or damaging it. By us-

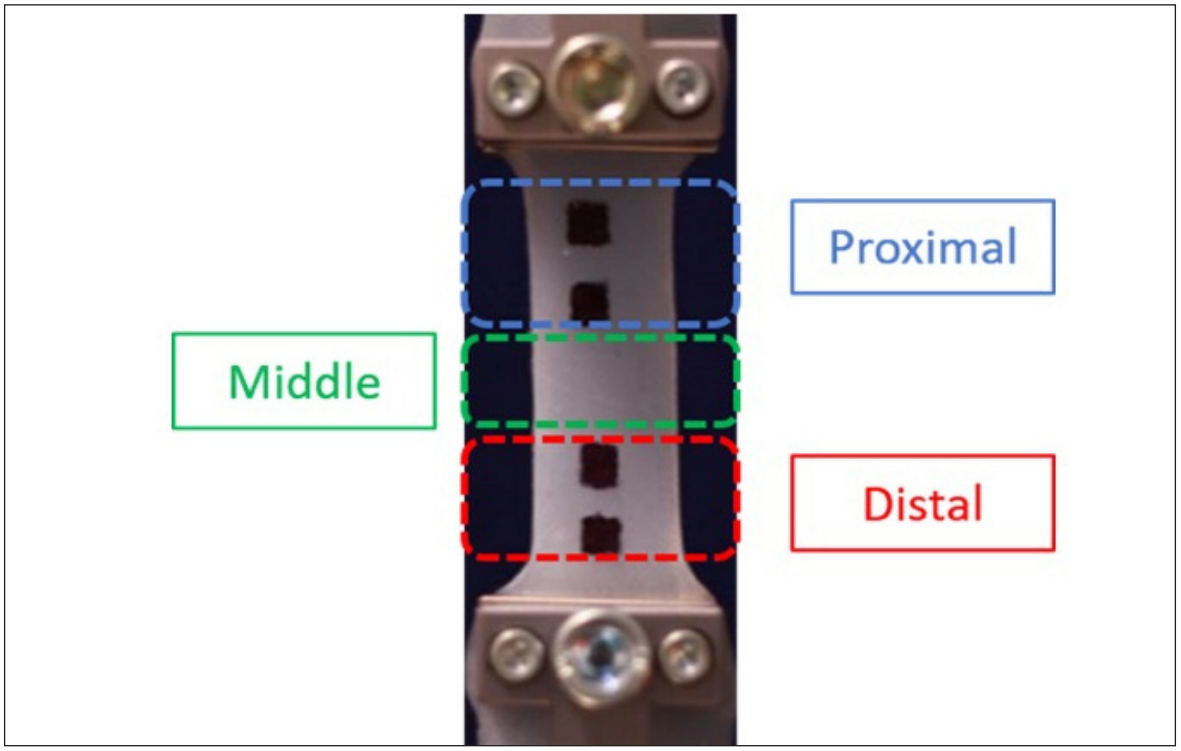

Figure 1. Dogbone specimen of the silicone material designed according to the ASTM D638 standard, clamped in the test bench machine. Four markers have been drawn on its surface. The principal regions of interest analyzed during the test are reported with different colors in the figure (proximal region in blue, middle region in green, distal region in red).

ing such drawn markers, it is possible to record the true displacement of the material during the tensile test. In fact, the measurements were free from potential errors arising from an eventual specimen slipping between the clamps. The markers allow to independently define and characterize different regions of interest of the same specimen at the same time. A set-up of the test is shown in Figure 1 in which the four markers identify three regions of interest that can simulate the regions close to the bony attachments and the middle region of a generic soft-tissue, as a ligament or tendon. Nevertheless, the markers can also be used to define any region in the structure even not adjacent.

A camera was fixed in front of the testing machine, enabling the continuous recording of the markers displacement during the entire experiment. The camera used was a Logitech C920. In order to remove any distortion effect, the camera was calibrated using OpenCV (Open Source Computer Vision Library, http://opencv.org) and a classical black-white chessboard. The images were then post-processed to remove any distortion. The camera was set to acquire up to 100 frames per test. Initially, the first experiment was based on the detection of circular marker. The results highlighted the necessity to change the shape of the markers as they could not be properly identified during the deformation. A quick trial showed that squared-shaped markers were better suited for the detection. They were drawn with a dark waterproof paint thus increasing the contrast with the specimen making them easily identifiable.

A dedicated user routine was developed to contactless automatically track the movements of the markers during the mechanical test.

Force outputs were continuously registered by the machine through a load cell of 10N (Nexygen Plus Software-Lloyd Instruments Ltd) during the uniaxial tensile test that can be perform with different crosshead speeds to simulate physiological conditions (Fig. 2). A preload of 5% of the maximum force value used during the test was applied to each specimen at the beginning of the test as suggested by previous researchers[22]. This prevented any irregularity due to a loose clamping of the sample. The values of the test considered for the results analysis were taken right after the preload phase was terminated.

By referring to a given dark background (Fig. 1), the camera can also provide the measurements of the changes in transversal section of the specimen, thus determining realistic changes of the cross-section area and giving the possibility to compute the Poisson's ratio. The automatic detection of the markers position was performed using the Icy software (http://icy.bioimageanalysis.org/).

The contactless method allowed to independently calculate the material properties for all regions of interest during the entire test. The length of the sample was defined as the distance between the centers of each couple of markers. The changes in thickness were correlated by the Log of the ratio between the transversal deformation and the longitudinal deformation. Hence, the user routine automatically obtained the true stress-strain curves and subdivided it in multiple regions. The value of the Young's modulus (E) and the Poisson's ratio (ν) were finally automatically computed for every region with Equations (1) and (2), respectively:

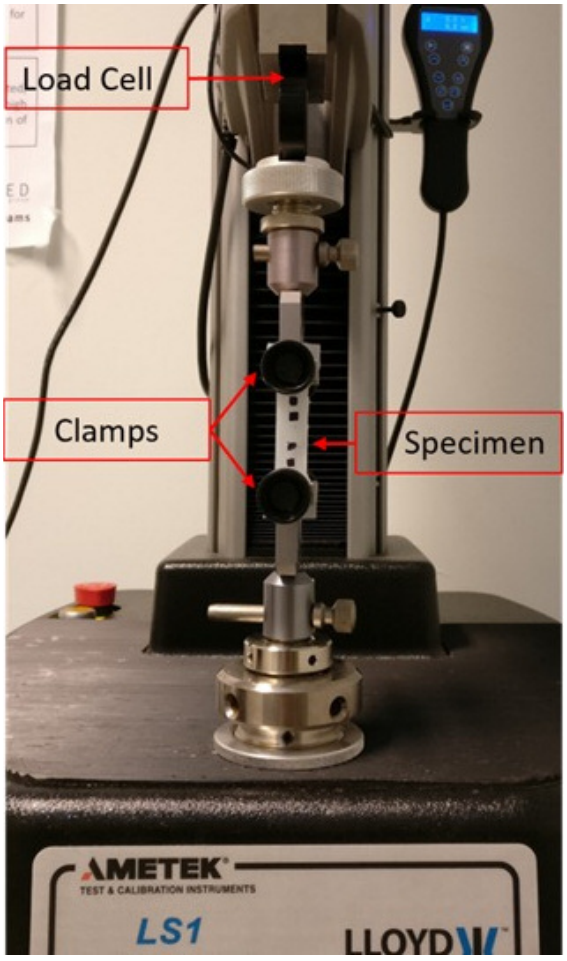

Figure 2. Traction test bench. The upper clamp is connected to a 10N load cell. The bottom clamp is fixed to the base of the machine. The sample is clamped using diamond coated jaws.

$$E = \frac{\sigma(\varepsilon)}{\varepsilon} \quad (1)$$

$$\nu = -\frac{\varepsilon_{tran}}{\varepsilon} (2)$$

where σ (MPa) is the tensile stress induced in the material, ε is the axial strain and ε_{tran} is the transverse strain of the material.

Verification of the repeatability and reproducibility of the procedure

The reliability of the procedure was initially tested analyzing the behavior of two specimens of a silicon material (Ecoflex 00-50, Smooth-On, Inc.) that were molded and tested under the same boundary conditions after four markers were drawn on them with similar position.

Based on the ASTM-D638 standard[23], the silicon samples were molded with a dogbone shape (Fig. 1).
On the obtained sample, the markers were drawn with different configurations (Fig. 3a). This strategy allowed to verify if the final material characterization could be dependent of the marker position and, by drawing multiple markers on the same sample, if it could be possible to characterize the behavior of different regions of the same sample. In particular:

- configuration 1, the markers were not vertically aligned and not equidistant;
- configuration 2, the markers were vertically aligned and not equidistant;
- configuration 3, the markers were vertically aligned and equidistant;
- configuration 4, the markers were not vertically aligned and equidistant.

Moreover, tracking the relative position of the extreme markers and the clamps of the machine would be possible to verify also potential sliding-effects of the sample and their amplitude.
Each specimen was clamped to the tensile machine and the tensile test was performed with a crosshead speed of 5 mm/min as recommended in the ASTM D638 standard[23]. The test was programmed to automatically stop after reaching a strain of 100%, corresponding to the double of the initial length of the specimen.
During the tests, the force and the markers displacement were continuously recorded. All the collected

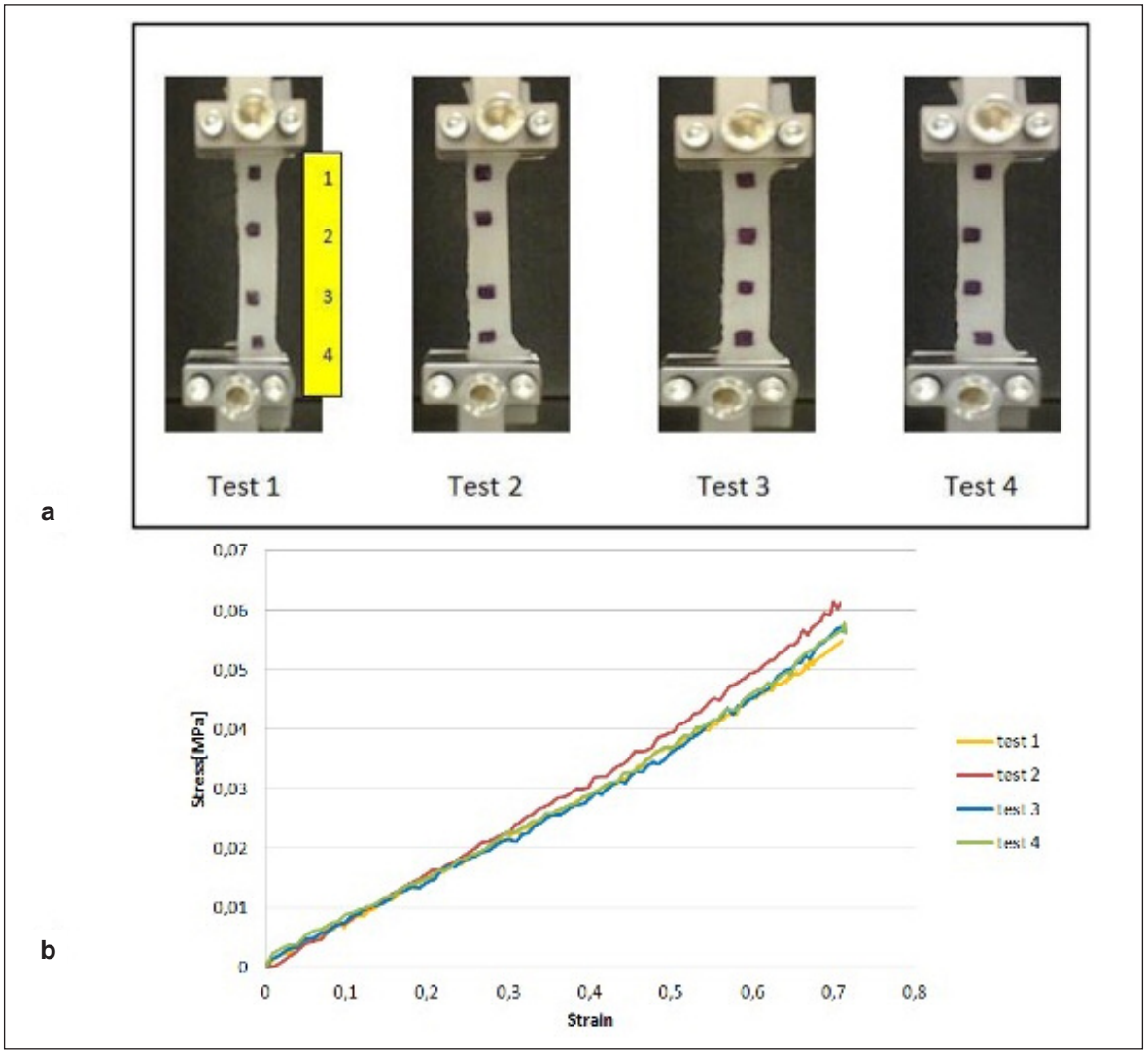

Figure 3 a, b. Analysis of the stress and strain measured using different markers position; a) configuration analyzed: in test 1 the markers are not vertically aligned and are not equidistant; in test 2 the markers are vertically aligned but not equidistant; in test 3 the markers are vertically aligned and equidistant; in test 4 the markers are not vertically aligned but equidistant. b) stress and strain curve measured by the central markers in the four configuration. Test 1, 3 and 4 are almost identical, test 2 show a slight change of the curve due to a higher distance among the markers.

data were later used together with the initial dimensions of the specimen and the position of the markers to calculate the pixels to millimeter scale factor. Each specimen was tested three times for the sake of repeatability. The same operator drew the markers on the two specimens and performed all tests.

Test on biological materials

Once the protocol was validated (details in "Results") the same set-up was applied to test biologic soft tissues. In particular, a fresh Achilles tendon of a pig was first tested to verify the feasibility of the procedure on biologic tissues. Then, a human patellar tendon was also used to calculate its material behavior and its variability.

The waterproof paint previously used on the synthetic material was also implemented for the biologic material. Despite the wet conditions of the material, the markers were patterned on the sample surface without any complication during the registration. The entire settings previously described were also implemented during these tests.

Results

The procedure resulted feasible for the chosen materials, both synthetic and biologic ones.

The use of the camera-tracking system for the contactless measure allows obtaining more accurate results than using the outputs of the tensile machine.

Figure 3b reported the analysis of the stress and strain measured using different markers positions as reported in Figure 3a. Results highlight how the configurations 1, 3 and 4 are almost identical, while test 2 shows a slight change of the curve due to a higher distance among the markers.

Figure 4 illustrates and compares the strain calculated by the clamp displacement (blue curve) and the strain determined by using the contactless approach (red curve for the middle region of the specimen and black curve for the overall region). Due to the presence of a sliding between the material and the clamps the length of the specimen determined by the machine is overestimated and, therefore, the strain (and the stress) calculated is higher than the real strain (and relative stress) of the material. In our test, there is an average difference of 32% between the stress obtained through the displacement of the clamps and the true stress computed through the proposed method. Comparing the true stress and true strain calculated by the contactless approach for the entire material and for the central region the average difference is of 1.25%.

Moreover, the user routine allows subdividing the curve of the material in several regions and a linear interpolation is obtained for each one of them (an example is illustrated in Fig. 5). For every selected subregion, the properties of the material were calculated. The error between the real curve and the interpolation can be immediately visualized and the operator can eventually decide to define different sub-regions.

Table I reports the calculated Young's modulus for two specimens in synthetic material. In particular, the measure has been repeated three times (each measure, the mean value and the standard deviations are reported).

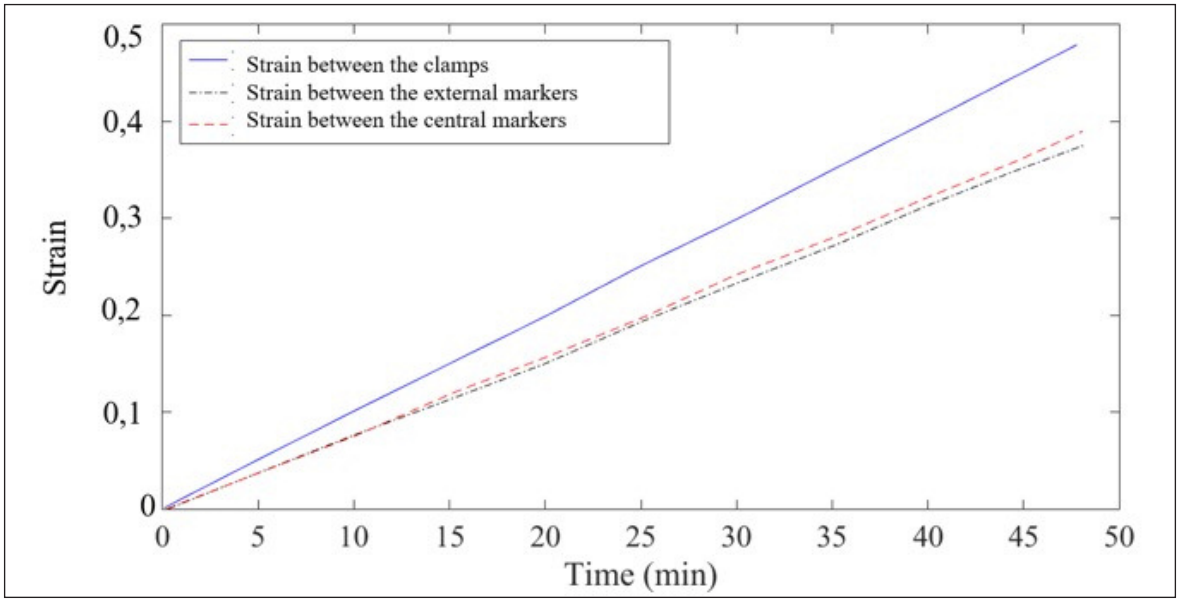

Figure 4. Comparison among the relative strain determined by the test machine (blue curve) and the strain determined by using the contactless approach (red curve for the strain the middle region of the specimen and black curve for the strain on the overall region). The blue curve is higher than the other two due to the sliding of the tissue on the clamp that will overestimate the specimen length.

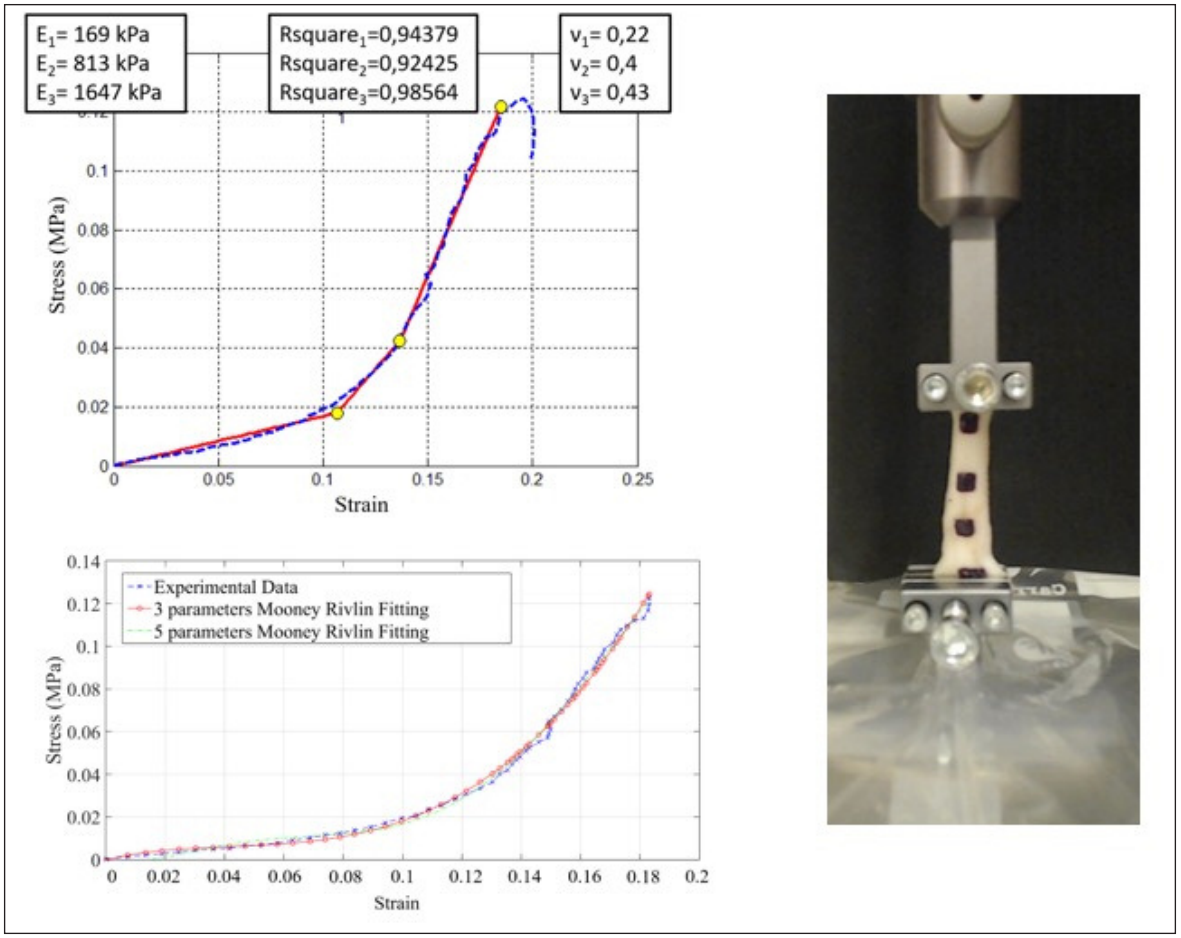

Figure 5. Example of a stress *vs* strain curve analysis on a pig Achilles tendon. The top figure shows an example of linear interpolation using 3 points to better discriminate the different regions of the curve. The boxes respectively show the Young's modulus (E), the error between the original trend and the interpolating lines (Rsquare), and the Poisson's ratio (v) for each segment of the stress/strain curve. The figure below illustrates the possibility of using the 3 parameters (red curve) and 5 parameters Mooney-Rivlin (green curve) curve fitting to approximate the experimental curve.

Table I. Mean value and standard deviation of the measured Young's modulus of two silicon specimens (each measurement was repeated three times).

		Mean E (MPa)	Standard Deviation (MPa)
Specimen 1	Central Markers	0.0922	0.00158
	External Markers	0.0945	0.000567
Specimen 2	Central Markers	0.108	0.00179
	External Markers	0.108	0.00169

Once the protocol for the synthetic material was applied, a maximum error of 3.7% has been estimated between the mean values computed for each specimen. Thus, the developed protocol can be considered trustable. Indeed, a difference between the mechanical properties of the material among the two different specimens exist and this change is due to the different production (in the lab) of the two dogbone specimens. In particular, two effects could explain this variability: first, the material used, second the mold adopted for the manufacturing of the specimen. In detail, the silicon used is a bi-component material and the mixing process of constituents was done manually, generating inhomogeneity in the final material used. Moreover, two molds were 3D printed using a 5th Generation Makerbot 3D printer (MakerBot In-

dustries, New York, USA) with an accuracy of 100 μm, therefore a possible change of the thickness of the sample of 0.1 mm could be foresee, changing the resistance of the final specimen.

The stress/strain curves of the three repetitions for each specimen have been compared. In particular, the analysis has been separately performed for the internal markers and the most external (middle region, and proximal and distal, respectively). The error has been calculated after linearly interpolating the real curve with respect to the mean value of the Young's modulus. The specimens recorded a mean error of 3.6% for the central markers, and 3.7% for external markers. Table I reports the outputs for the two specimens for the three repetitions. The mean values of the Young's modulus computed for the central markers and the external markers differ by 2% and 0% respectively for the specimen 1 and 2. The automatic procedure results reliable to accurately determine the Young's modulus in every selected region with an average accuracy of 1,25%.

Hence, the procedure is not only feasible and realistic, but it is also reliable without any impact due to the intervention of the operator.

An interpolation procedure, where the operator choses 3 points of the curve, allows the operator to split the stress/strain curve. The algorithm then automatically calculates the two linear segments best fitting to the experimentally obtained results. The Young's modulus as well as the Poisson's ratio are then calculated for each segment. The R-square statistical value quantifies the fitting quality of the interpolation. The closest this value is to 1, the best is the fitting.

The tensile test on the Achilles tendon was led up to the rupture of the soft-tissue and the obtained characterization is depicted in Figure 5. The rupture stress was measured around 0.12 MPa for an elongation of approximately 20%. Based on the experimental results obtained, the 3 parameters and 5 parameters Mooney-Rivlin model was used to approximate the characteristics of the pig's Achilles tendon as shown in Figure 5. Both the 3 and 5 parameters models allow a good approximation with a value of the squared two-norm of the residual of the order of magnitude of 10^{-4}.

Figure 6 reported the average Stress-Strain curve determined by a tensile test on a human patellar tendon and the relative standard deviation. Results clearly illustrate the low variability of the results among the different repetitions. In particular, the patellar tendon is characterized by an initial non-linear toe-region (up to strain of 1%), where large strains produce only small stress; the quasi-linear region, where the stress-strain curve is approximately linearly elastic and the failure region (after strain of 7.5%), where the Young's modulus decrease as collagen fibers become damaged and fractured[20,21].

Discussion

Univocal guidelines for the characterization of soft-tissue material properties are currently lacking in the literature. However, this information can be very useful for several players, as researcher, clinician and medical industry oriented to develop artificial soft-tissues or medical devices. For this reason, this study is focused on the development and validation of a repeatable and reproducible testing protocol enabling the mechanical characterization of soft-tissue materials. The proposed protocol automatically computes the

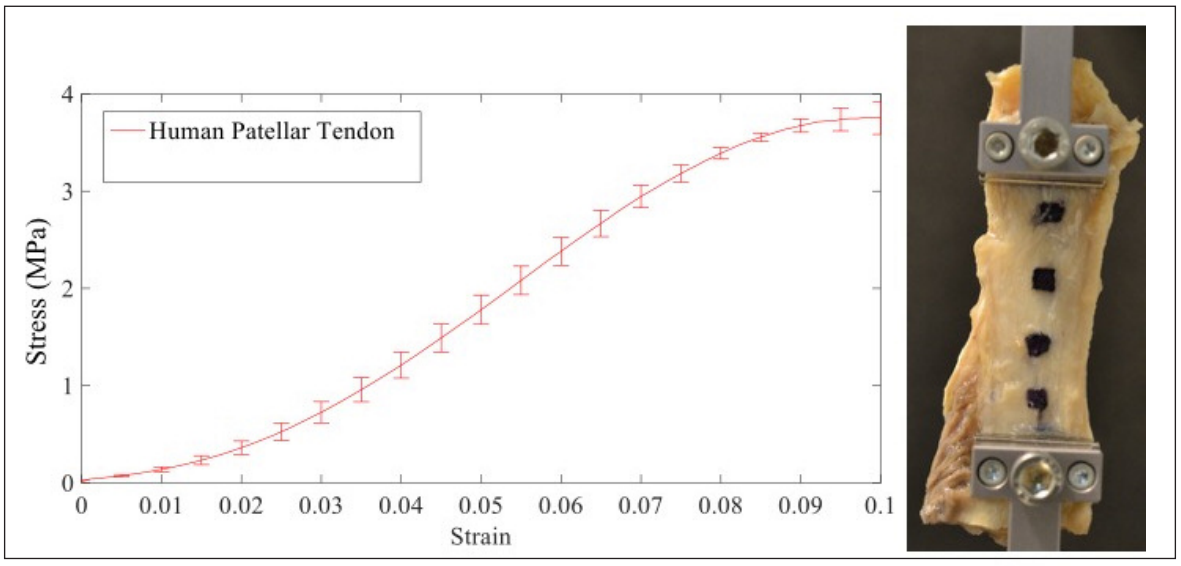

Figure 6. Average stress *vs* strain curve determined by a tensile test on a human patellar tendon and relative standard deviation.

Young's modulus and the Poisson's ratio of the specimen. Moreover, this information can be automatically obtained for different regions of interest of the same specimen. Additionally, linear interpolations on subregions of the mechanical trend of the curve allow computing different characteristics of the material behavior (toe-region/elastic region/failure). The procedure has been first calibrated on a silicone material with a maximum error of <4% in terms of Young's modulus variability.

The use of the markers for the material characterization, instead of the testing machine outputs, allows to make the test independent from the residual equipment deficiencies/errors. Moreover, the number and position of the markers do not affect the final results of the soft tissue characterization for similar regions of interest.

The choice of the points is operator-dependent. An expert operator was able to identify from one to three best fitting points for the interpolation procedure, proving that more points allow a more accurate interpolation. However, if the operator is not an expert, the choice of a single point leads to a reasonable good approximation of the curve and limits the errors dependent by the operator.

The procedure has also been tested for biologic soft tissues, both animal and human, with excellent results, thus looking promising for other soft-tissue samples.

The proposed procedure can be used for several applications, for example, generating a full database of soft-tissues materials properties and behaviors. Operators of the numerical community that tackle with soft-tissues modeling for several applications[4,24,25] could then refer to such kind of database. Thus, collected data could be updated with respect to what can be found in the literature. The new collected information can consecutively support new surgical treatments and biomechanical implementations.

Further improvements in the technique would be the implementation of a second camera, placed orthogonally to let the procedure estimating the changes in the specimen section and accurately recording the out-of-plane marker motions.

Conclusion

In this study, a procedure to accurately and automatically determine material properties in soft-tissues was developed, tested, and applied during uniaxial tensile tests. The proposed technique was suitable in characterizing a given material with an error lower than 4% (and with high reproducibility and repeatability). Such technique, applied for biologic animal and human samples resulted verified, thus could be easily extended for the characterization of other biologic materials.

Ethics

The Authors declare that this research was conducted following basic ethical aspects and international standards as required by the journal and recently update in[26].

References

1. Nordin M, Frankel VH. Basic Biomechanics of the Musculoskeletal System. Lippincott Williams & Wilkins. 2001.
2. Korhonen RK, Saarakkala S. Biomechanics and Modeling of Skeletal Soft Tissues. Theor Biomech. 2011;113-132.
3. Pianigiani S, Labey L, De Corte R, Pascale W. Mechanical Characterization of the Soft Tissues of a Native Human Knee: A Pilot Study. J Sport. Sci. 2014;2:173-180.
4. Pianigiani S, Innocenti B. The use of finite element modeling to improve biomechanical research on knee prosthesis. In: New Developments in Knee Prosthesis Research. 2015;113-125.
5. Galbusera F, Freutel M, Dürselen L, D'Aiuto M, Croce D, Villa T, Sansone V, Innocenti B. Material models and properties in the finite element analysis of knee ligaments: a literature review. Front. Bioeng. Biotechnol. 2014;2:54.
6. Woo SLY, Abramowitch SD, Kilger R, Liang R. Biomechanics of knee ligaments: Injury, healing, and repair. J. Biomech. 2006;39:1-20.
7. Butler DL, Guan Y, Kay MD, Cummings JF, Feder SM, Levy MS. Location-dependent variations in the material properties of the anterior cruciate ligament. J Biomech. 1992;25:511-518.
8. Chandrashekar N, Mansouri H, Slauterbeck J, Hashemi J. Sex-based differences in the tensile properties of the human anterior cruciate ligament. J Biomech. 2006;39:2943-2950.
9. Kwon OS, Purevsuren T, Kim K, Park WM, Kwon TK, Kim YH. Influence of bundle diameter and attachment point on kinematic behavior in double bundle anterior cruciate ligament reconstruction using computational model. Comput. Math. Methods Med. 2014:2014.
10. Noyes FR, Grood ES. The strength of the anterior cruciate ligament in humans and Rhesus monkeys. J. Bone Joint Surg. Am. 1976;58:1074-1082.
11. Prietto MP, Bain JR, Stonebrook SN, Settlage RA. Tensile strength of the human posterior cruciate ligament (PCL). In Transactions of the annual meeting of the Orthopaedic Research Society. 1988;13:736-745.
12. Race A, Amis A. The mechanical properties of the two bundles of the human posterior cruciate ligament. J Biomech. 1994;27:13-24.
13. Ramaniraka NA, Saunier P, Siegrist O, Pioletti DP. Biomechanical evaluation of intra-articular and extra-articular procedures in anterior cruciate ligament reconstruction: A finite element analysis. Clin. Biomech. 2007;22:336-343.
14. Butler DL, Kay MD, Stouffer DC. Comparison of material properties in fascicle-bone units from human patellar tendon and knee ligaments. J Biomech. 1986;19:425-432.
15. Blankevoort L, Huiskes R. Ligament-bone interaction in a three-dimensional model of the knee. J Biomech. Eng. 1991;113:263-269.
16. Robinson JR, Bull AMJ, Amis AA. Structural properties of the medial collateral ligament complex of the human knee. J Biomech. 2005;38:1067-1074.
17. Shelburne KB, Pandy MG. A musculoskeletal model of the knee for evaluating ligament forces during isometric contractions. J Biomech. 1997;30:163-176.
18. Stäubli HU, Schatzmann L, Brunner P, Rincón L, Nolte LP. Mechanical tensile properties of the quadriceps tendon and patellar ligament in young adults. Am. J Sports Med. 1999;27:27-34.
19. Woo SL, Hollis JM, Adams DJ, Lyon RM, Takai S. Tensile

properties of the human femur-anterior cruciate ligament-tibia complex. The effects of specimen age and orientation. Am. J Sports Med. 1991;19:217-225.
20. Bartel DL, Davy DT, Keaveny TM. Orthopaedic Biomechanics: Mechanics and Design in Musculoskeletal Systems. 1st ed. New Jersey: Pearson Prentice Hall. 2006.
21. Woo SL, Debski SE, Withrow JD, Janaushek M. Biomechanics of knee ligaments. Am. J Sports Med. 1999;27:533-543.
22. Innocenti B, Bilgen ÖF, Labey L, Van Lenthe GH, Vander Sloten J, Catani F. Load sharing and ligament strains in balanced, overstuffed and understuffed UKA. A validated finite element analysis J. Arthroplasty. 2014;29:1491-1498.
23. ASTM International, "Standard test method for tensile properties of plastics," ASTM Int. 2003;8:46-58.
24. Innocenti B, Pianigian S, Ramundo G, Thienpont E. Biomechanical Effects of Different Varus and Valgus Alignments in Medial Unicompartmental Knee Arthroplasty. J of Arthroplasty. 2016;31:2685-2691.
25. Pianigiani S, Labey L.Pascale W, Innocenti B. Knee kinetics and kinematics: What are the effects of TKA malconfigurations? KSSTA. 2016;24:2415-2421.
26. Padulo J, Oliva F, Frizziero A, Maffulli N. Muscles, Ligaments and Tendons Journal - Basic principles and recommendations in clinical and field science research: 2016 update. MLTJ. 2016;6(1):1-5.